Journal of Pharmaceutical and Biomedical Analysis 70 (2012) 158–168

Contents lists available at SciVerse ScienceDirect

Journal of Pharmaceutical and Biomedical Analysis

journal homepage: www.elsevier.com/locate/jpba

Analysis of recombinant monoclonal antibodies by RPLC: Toward a generic method development approach

Szabolcs Fekete[a,*], Serge Rudaz[a], Jenő Fekete[b], Davy Guillarme[a]

[a] School of Pharmaceutical Sciences, University of Geneva, University of Lausanne, Boulevard d'Yvoy 20, 1211 Geneva 4, Switzerland
[b] Budapest University of Technology and Economics, Department of Inorganic and Analytical Chemistry, Szt. Gellért tér 4, Budapest 1111, Hungary

ARTICLE INFO

Article history:
Received 24 April 2012
Received in revised form 29 May 2012
Accepted 15 June 2012
Available online 23 June 2012

Keywords:
Monoclonal antibodies
Core–shell
UHPLC
DryLab
Method development
Optimization software

ABSTRACT

Monoclonal antibodies (mAbs) are an emerging class of therapeutic agents that have recently gained importance. To attain acceptable kinetic performance with mAbs in reversed phase liquid chromatography, there is a need to work with the last generation of wide-pore sub-2 μm fully porous or core–shell particles stationary phases. In addition, temperature in the range 60–90 °C was found to be mandatory to limit adsorption phenomenon of mAbs and their fragments. A generic method development strategy was proposed to account for the selectivity, efficiency, recovery, and the possible thermal degradation. This study also demonstrated that the gradient steepness and temperature cannot be optimized using van't Hoff type linear models. Similarly, the common linear solvent strength model also generated some error in predicting the retention times. In contrast, when quadratic models were employed, the prediction accuracy of retention times was found to be excellent (relative error between 0.5 and 1%) using a reasonable number of experiments (9 or 6 experiments for optimization of gradient time and temperature, which requires between 6 and 8 h). Two separations of mAbs fragments were performed to demonstrate the reliability of the quadratic approach.

1. Introduction

It has been demonstrated that reverse-phase liquid chromatography (RPLC) is one of the most promising analytical techniques in the field of peptide and protein analysis [1,2]. The efficiency obtained with RPLC is generally superior to that of ion-exchange (IEX) or size-exclusion (SEC) chromatography [1]. Furthermore, the separation time can be considerably shortened with RPLC compared to IEX or SEC. Another advantage is the straightforward coupling of this technique to various ionization methods for mass spectrometry (MS) detection.

In laboratory applications (e.g., biopharmaceutical quality control, industrial issues), separations of proteins with very similar molecular weights and nearly identical structures (conformations) are often performed. Very often, the difference in physicochemical properties is relatively small and therefore similar retention behaviors are expected for the different forms. In many cases, selectivity cannot be improved, so efficiency must be increased to enhance the resolution. Therefore, the stationary phase and temperature become the two most relevant parameters in method development. By using the most advanced stationary phases, such as core–shell type materials, sub-2 μm porous particles or wide-pore monolithic columns, the separation power can be increased considerably [3–7]. A recent systematic study demonstrated the effect of column length on peak capacity of intact protein separations [8].

The number of approved monoclonal antibodies (mAbs) has been growing continuously in the pharmaceutical field. Antibodies are large tetrameric glycoproteins of approximately 150 kDa, composed of four polypeptide chains: two identical heavy chains (≈50 kDa) and two identical light chains (≈25 kDa) that are connected through several inter- and intra-chain disulfide bonds at the hinge region. The resulting tetramer has two similar halves that form a Y-like shape [9]. Functionally, mAbs consist of two regions: the crystallizable fraction (Fc) and the antigen-binding fraction (Fab) [10]. Because this structure is made of four polypeptide chains, monoclonal antibodies can display considerable micro-heterogeneity. There are several common modifications that produce charge variants (or isoforms) (e.g., deamidation, C-terminal lysine truncation, N-terminal pyroglutamation, methionine oxidation, and glycosylation variants) and size variants of the peptide chains (e.g., aggregation or incomplete formation of disulfide bridges). Due to the increasing importance of this class of therapeutic compounds, the development of analytical methods for their detailed characterization is an active area of study. Complete proteolytic digestion of mAbs (peptide mapping) followed by gradient RPLC/MS analysis is the method of choice for

* Corresponding author. Tel.: +41 22 37 963 34; fax: +41 22 379 68 08.
E-mail addresses: szfekete@mail.bme.hu, szabolcs.fekete@unige.ch (S. Fekete).

0731-7085/$ – see front matter © 2012 Elsevier B.V. All rights reserved.
http://dx.doi.org/10.1016/j.jpba.2012.06.021

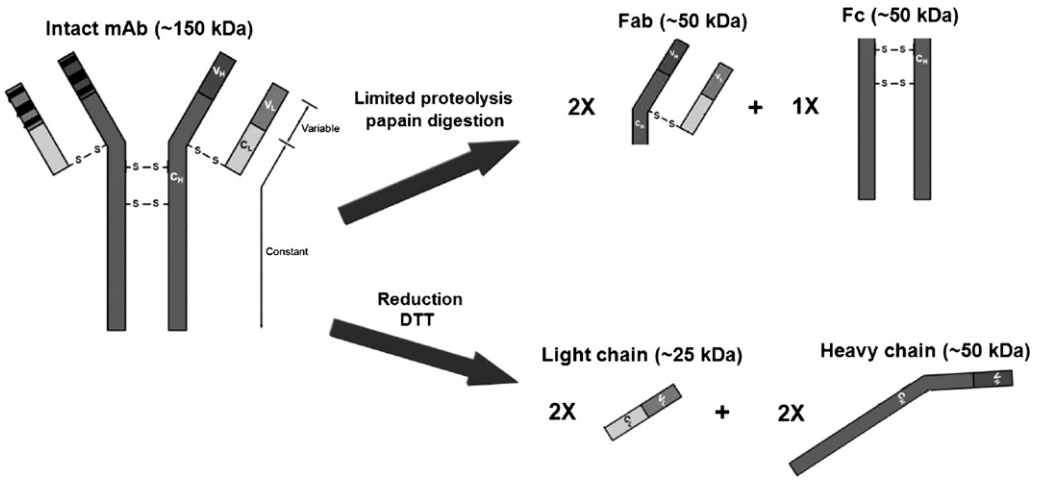

Fig. 1. Schematic view of the limited proteolytic digestion and reduction of monoclonal antibodies.

the identification and quantification of chemical modifications of mAbs [11,12]. However, peptide mapping is time consuming and can induce putative modifications during the lengthy and complex sample preparation [12]. Alternatively, the analysis of large mAb fragments, such as Fab, Fc, $F(ab')_2$, HC and LC, requires very little sample preparation and can provide a high-throughput alternative to peptide mapping (the sample preparation procedure of mAb fragments is summarized in Fig. 1). For these reasons and due to advances in RPLC columns and instrumentation, the second approach is currently preferred over the traditional peptide mapping.

In the development of RPLC methods for small molecule characterization, computer modeling programs are employed to improve the analytical throughput and obtain detailed information about method specificity. The most successful and widespread modeling program (DryLab, Molnar-Institute, Berlin, Germany) optimizes the Design Space by measuring and visualizing the effect of different parameters including mobile phase composition, gradient time and shape, pH, ionic strength, ternary eluent, additive concentrations or temperature [13]. For this purpose, the program suggests a relatively well-defined number of experiments for a particular stationary phase. Furthermore, it can predict the separation inside the Design Space based on changes in the mobile phase composition, mode of elution (either isocratic or gradient), temperature, and pH, as well as column parameters such as column length, internal diameter, particle size and flow rate [14]. In the case of large biomolecules, such as mAbs, conformational changes in proteins that occur in response to varying chromatographic conditions could be very complex, leading to unpredictable behavior based on the chemical-chromatographic relationship (e.g., LSS theory). Thus, there is a need to evaluate the validity of the models employed by the software.

This study took advantage of the recently commercialized and very efficient columns packed with either wide-pore sub-2 μm, fully porous stationary phase or the last generation core–shell particles. The retention properties of large mAb fragments were investigated. Selectivity, efficiency and possible thermal degradations were all considered and a generic method development approach was proposed. The commonly used linear retention models (linear solvent strength or van't Hoff models) were modified into quadratic models, resulting in very accurate prediction of the retention times. Moreover, the goal of this study was the evaluation of method optimization software such as DryLab for the separation of antibody fragments by using customized models during the optimization process. This new approach allows a very fast and accurate systematic method development for the efficient separation of mAbs fragments.

2. Experimental

2.1. Chemicals and columns

Acetonitrile (gradient grade) was purchased from Sigma–Aldrich (Buchs, Switzerland). Water was obtained with a Milli-Q Purification System from Millipore (Bedford, MA, USA).

IgG monoclonal antibodies, including rituximab (MabThera) and bevacizumab (Avastin), were purchased from Roche (Roche Pharma, Switzerland), and panitumumab (Vectibix) was purchased from Amgen (Switzerland). For the fragmentation of monoclonal antibodies, dithiothreitol (DTT) and papain (from Carica papaya) were obtained from Sigma–Aldrich (Buchs, Switzerland). Trifluoroacetic acid (TFA) was purchased from Sigma–Aldrich (Buchs, Switzerland).

Acquity BEH300 C18 and C4 columns with a particle size of 1.7 μm (150 mm × 2.1 mm, 300 Å) were purchased from Waters (Milford, MA, USA). An Aeris Widepore (WP) C18 column packed with 3.6 μm core–shell particles (150 mm × 2.1 mm) was a generous gift from Phenomenex Inc. (Torrance, CA, USA).

2.2. Equipment and software

All measurements were performed using a Waters Acquity UPLC™ system equipped with a binary solvent delivery pump, an autosampler and a UV and/or fluorescence (FL) detector. The Waters Acquity system includes a 5 μl sample loop and a 0.5 μl UV flow-cell and a 2 μl FL flow-cell. The loop is directly connected to the injection switching valve (no needle seat capillary). The connection tube between the injector and column inlet was 0.13 mm I.D. and 250 mm long (passive preheating included), and the capillary located between the column and detector was 0.10 mm I.D. and 150 mm long. The overall extra-column volumes (V_{ext}) were approximately 13 μl and 15 μl, as measured from the injection seat of the auto-sampler to the UV and FL detector cells, respectively. The measured dwell volume was approximately 100 μl. Data acquisition and instrument control was performed using the Empower Pro 2 Software (Waters). Calculation and data transfer were achieved using Excel templates.

Method optimization was performed using DryLab® 2010 Plus chromatographic modeling software (Molnar-Institute, Berlin, Germany).

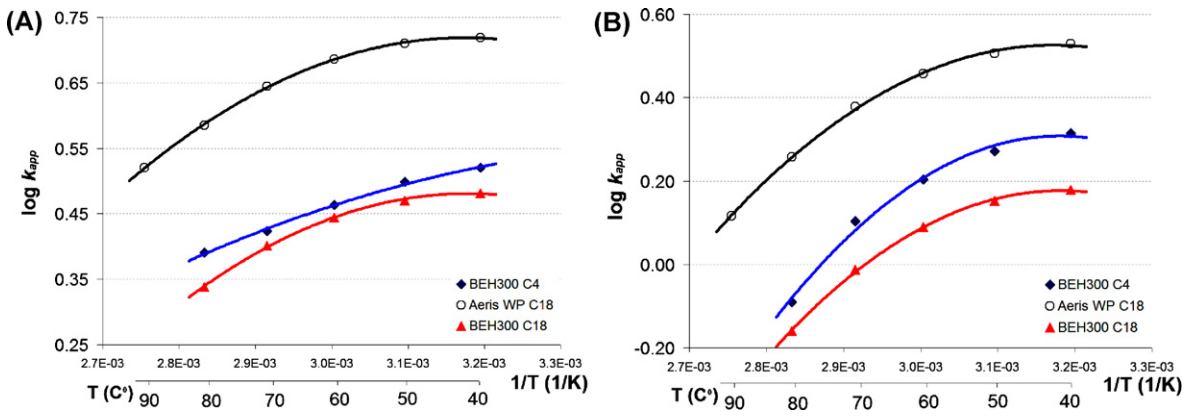

Fig. 2. The effect of temperature (and stationary phase) on the apparent gradient retention factor of rituximab heavy chain (A) and light chain (B) fragments. Columns: Aeris WP C18, Acquity BEH300 C18 and C4 (150 mm × 2.1 mm), injected volume: 0.5 μl, detection: fluorescence (excitation at 280 nm, emission at 360 nm). Mobile phase A: 0.1% TFA in water, mobile phase B: 0.1% TFA in acetonitrile. Gradient: from 30% to 37% B on the Aeris WP C18 and BEH300 C4 columns, and from 32% to 39% on the BEH300 C18 column in 6 min, flow rate: 0.3 ml/min. Temperature was varied from 40 to 80 °C on the BEH300 columns and from 40 to 90 °C on the Aeris WP C18 column.

2.3. Apparatus and methodology

2.3.1. Mobile phase composition and sample preparation

For the gradient separation of mAbs and its fragments, the mobile phase "A" consisted of 0.1% TFA in water, whereas the mobile phase "B" was 0.1% TFA in acetonitrile.

The intramolecular disulfide bonds of IgG monoclonal antibodies were reduced using DTT. For this purpose, 0.05 mg of DTT was added to 100 μl of a concentrated mAb solution and incubated at 30 °C for 60 min. Proteins were completely converted into the light and heavy chain components.

The digestion of rituximab and bevacizumab was initiated by the addition of papain (diluted to 100 μg/ml in water) to reach a final protein:enzyme ratio of 100:1 (m/m%). The digestion was carried out at 37 °C for 3 h. The final digestion volume of 200 μl was directly injected using low volume insert vials.

2.3.2. Investigation of retention properties of antibody fragments

Heavy chain, light chain, Fab and Fc fragments of rituximab, bevacizumab and panitumumab were eluted in the gradient mode.

To investigate the effect of temperature (Fig. 2), short gradient runs (6 min) were performed on the three columns at different temperatures from 40 °C to the upper temperature limit of the column (in 10 °C steps). The BEH300 C4 and C18 materials are stable up to 80 °C, whereas the Aeris WP C18 is stable up to 90 °C (according to the vendors). Although the recovery of mAb fragments is not acceptable at 40 and 50 °C, our purpose was to illustrate the effect of temperature on the retention times using a relatively broad range of temperatures. Setting the mobile phase temperature to less than 60 °C is not effective for the separation of these large fragments.

For the rituximab samples, a linear gradient from 30 to 37% B was employed with the Aeris WP C18 and BEH300 C4 columns, whereas with the BEH300 C18 column, the gradient was varied from 32 to 39% B to maintain a similar apparent gradient retention factor. Because panitumumab is slightly more hydrophobic than rituximab, the gradient programs were adjusted to achieve comparable apparent retention properties. For the panitumumab samples, a linear gradient from 31 to 39% B was employed with the Aeris WP C18 and BEH300 C4 columns, whereas a gradient of 33 to 41% B was used with the BEH300 C18 column. For the bevacizumab samples, a generic gradient of 31 to 40% B provided suitable retention times for all three columns. In this study, short gradient separations (6 min on 15-cm long columns) were utilized to avoid any possible thermal degradation of the samples at elevated temperatures. The flow rate was set to 0.3 ml/min. The chromatograms were recorded in both UV (215 nm) and fluorescence mode (excitation at 280 nm, emission at 360 nm). The retention properties on the different stationary phases were evaluated by plotting the logarithm of the apparent gradient retention factors ($\log k_{app}$) as a function of $1/T$ (reciprocate temperature).

To evaluate the effect of gradient steepness on the retention properties (Fig. 3), different gradient times were tested at a given temperature. A generic linear gradient, starting from 30% to 40% B, was employed at a flow rate of 0.35 ml/min for all samples. The gradient time was varied from 4, to 8, 12 and 16 min (at 70 and 90 °C). Both UV and fluorescence detection modes were used. The observed $\log(k_{app})$ values were plotted as a function of the logarithm of gradient time.

2.3.3. Systematic method optimization

Snyder and co-workers demonstrated the utility of initial basic runs for multifactorial experimental designs in 1990s [15]. The general approach is to simultaneously model the effect of temperature and gradient steepness on the selectivity of a previously selected RP column [16,17]. For conventional standard bore columns (I.D. of 4.6 mm) with a length of 15 and 25 cm, at 1–2 ml/min flow rate with a 5–100% ACN-water gradient, two gradients of tg_1 = 20–30 min and tg_2 = 60–90 min should be employed to obtain accurate predictions from the linear solvent strength (LSS) model. The modeling software is then used to generate resolution maps that show the critical resolution of the separated peaks [18]. In this manner, the gradient program and column temperature can be rapidly and efficiently optimized.

Recent studies have showed that mAb fragments (IgG1 and IgG2) generally elute using a 30–40% ACN (containing 0.1% TFA) gradient at elevated temperatures [4,19]. In ultra high-pressure liquid chromatography (UHPLC), narrow bore columns (2.1 mm I.D.) are generally used to increase the sensitivity, reduce frictional heating effects and decrease the solvent and sample consumption. By taking into account the fact that (i) only a 10% change in B produces an adequate gradient for eluting all the different mAb fragment variants and (ii) that 2.1-mm columns are used; then applying the rules of geometrical method transfer [13,20], the following conclusions can be drawn. For 150 mm × 2.1 mm columns, gradient times in the range of tg_1 = 4 min to tg_2 = 12 min (at a flow rate of 0.35 ml/min, starting from 30 to 40% B) should provide appropriate initial data for constructing resolution maps and predicting retention times.

It was recently demonstrated [19] that the use of elevated temperatures (up to 80–90 °C) is necessary for the RPLC separation of mAb fragments due to the adsorption phenomena on both

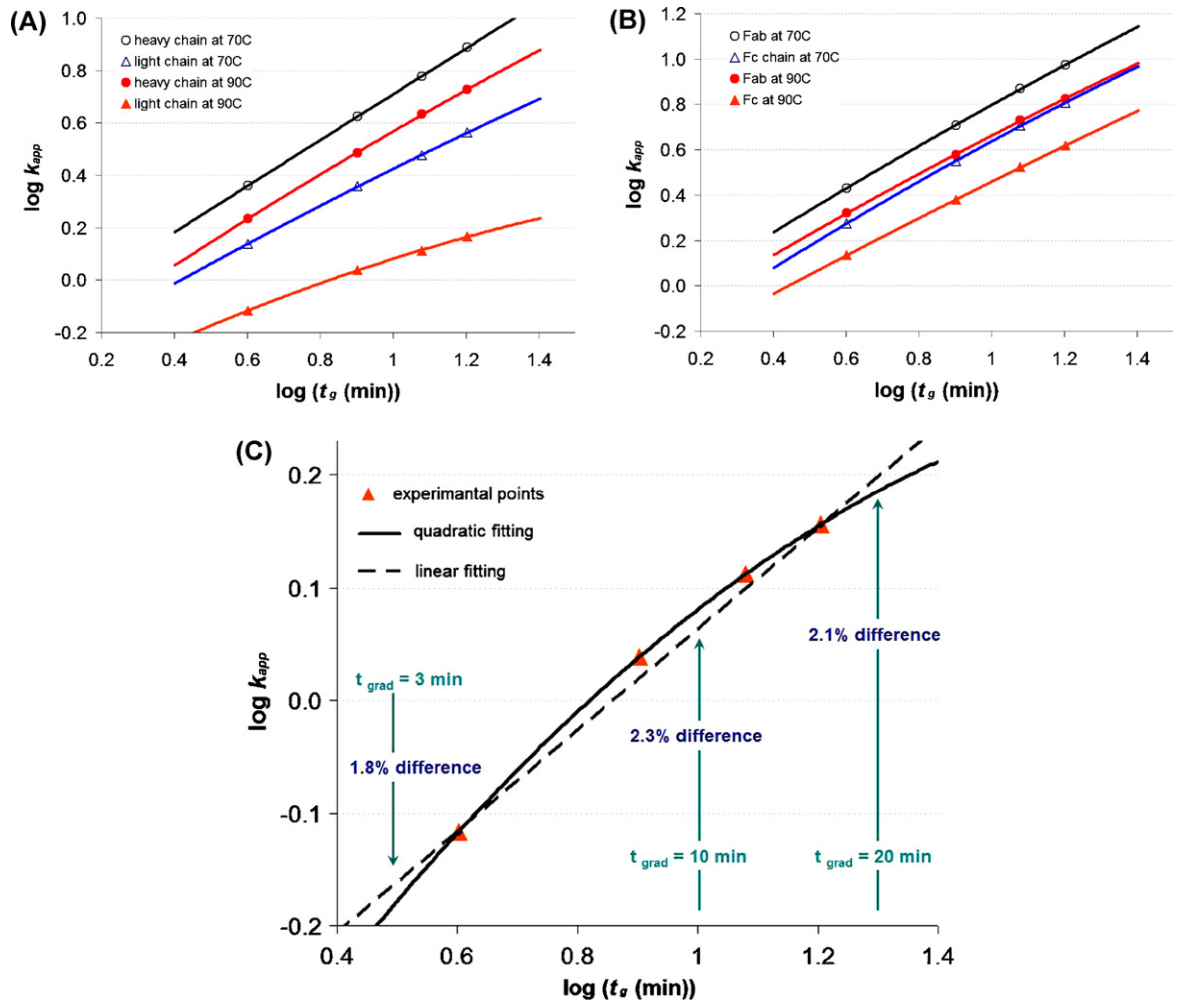

Fig. 3. The effect of gradient time (at a given temperature) on the apparent gradient retention factor of rituximab heavy chain and light chain fragments (A), and of bevacizumab Fc and Fab fragments (B) and the deviation between linear and quadratic fitting in case of the rituximab light chain (C). Column: Aeris WP C18 (150 mm × 2.1 mm), injected volume: 0.5 μl, detection: fluorescence (excitation at 280 nm, emission at 360 nm). Mobile phase A: 0.1% TFA in water, mobile phase B: 0.1% TFA in acetonitrile. Gradient: from 30% to 40% B, flow rate: 0.35 ml/min. The gradient time (steepness) was varied as 4, 8, 12 and 16 min (at 70 and 90 °C).

silica-based and hybrid stationary phases. At elevated temperatures, thermal degradation is possible and becomes relevant for gradient times longer than 20 min [19]. A compromise must be found between the residence time and separation temperature. Therefore, the use of $tg_1 = 4$ min and $tg_2 = 12$ min gradients were employed to avoid issues with stability. Finally, the effect of temperature on selectivity and resolution should be investigated only in a limited temperature range (e.g., $\Delta T = 20$ °C). The mobile phase temperature should thus be set to $T_1 = 70$ °C and $T_2 = 90$ °C (or $T_1 = 60$ °C and $T_2 = 80$ °C depending on the thermal stability of the stationary phase).

As discussed in Section 3, because linear models cannot be used to describe the behavior of large biomolecules (25–50 kDa), quadratic models were applied for the optimization. A 3^2 factorial design was chosen to simultaneously optimize the gradient steepness and mobile phase temperature. The effect of the two factors was investigated at 3 levels. Gradient time was equidistantly set to $tg_1 = 4$ min, $tg_2 = 8$ min and $tg_3 = 12$ min while temperature was set to $T_1 = 70$ °C, $T_2 = 80$ °C and $T_3 = 90$ °C. Two examples demonstrate the reliability of the second-degree polynomial model. The first example shows the optimization process for the RPLC separation of bevacizumab Fc and Fab fragments (Section 3.3.1), whereas the second example confirms the accuracy of this approach when applied to the separation of the light chain and heavy chain variants of rituximab (Section 3.3.2).

3. Results and discussion

When dealing with low molecular weight analytes, the most common strategy in method development consists of selecting a suitable stationary phase chemistry, organic modifier and mobile phase pH. The gradient program and mobile phase temperature are subsequently tuned as complementary parameters for a second level optimization.

In the case of large biomolecules such as mAb fragments, the method development rules are different and some additional constraints should be considered. First, a highly efficient wide-pore stationary phase must be used, but the chemistry of such columns is very limited and only a small number of C4, C8 or C18 materials are currently available. To attain suitable peak shapes with maximum efficiency, the mobile phase containing 0.1% TFA is typically recommended. Finally, acetonitrile should be selected as the solvent because it provides a lower backpressure when using columns packed with sub-2 μm particles, in comparison with methanol or isopropanol, and is particularly favorable in terms of kinetic performance.

Based on these considerations, this study was conducted using recently developed stationary phases, namely, the Acquity BEH300 and Aeris Widepore C4 or C18, and a mobile phase consisting of water with 0.1% TFA and acetonitrile with 0.1% TFA. The mobile phase temperature and gradient steepness

were optimized to achieve the optimum separation of the mAb fragments.

3.1. Retention behavior of antibody fragments

3.1.1. Effect of temperature on the retention properties

In RPLC, the effect of temperature on the retention factor (k) can generally be expressed by the van't Hoff equation:

$$\log k = -\frac{\Delta H}{RT} + \frac{\Delta S}{R} + \log \beta \quad (1)$$

where ΔH is the enthalpy change associated with the transfer of the solute between phases, ΔS is the corresponding entropy change, R is the molar gas constant, T is the absolute temperature and β is the phase ratio of the column. When $\log(k)$ is plotted against $1/T$, the enthalpy is calculated from the slope of the curve. With neutral compounds, the van't Hoff plots exhibit a linear relationship. However, a quadratic dependence of $\log(k)$ versus $1/T$ was observed over a wide range of temperatures in another study [21], which employed silica and non-silica based stationary phases (this phenomenon has not been fully explained yet). The effect of temperature on the retention of partially ionized compounds that exist in two forms can also be described by Eq. (1). However, both enthalpy and entropy are expected to be different for the two forms (i.e., molecular and ionized forms); as a result, both H and S can vary with temperature when both forms are present in significant quantities [21]. Melander et al. [22] and Castells et al. [23] have developed complex relationships to describe the retention behavior of a partially ionized solute with a unique acid–base equilibrium, based on the assumption that the retention factor is considered as the weighted average of the retention factors of the individual forms.

The effect of temperature on the retention behavior becomes more complex for large biomolecules. Depending on the stability of the secondary structure, the molecules unfold to a different extent and interact with the stationary phase with varied strength [24]. Due to the different conformation-dependent response of proteins at elevated temperatures, the change in the retention times can be very different [25,26]. Therefore, temperature offers the ability to adjust the selectivity of the separation. If a protein is completely denatured into a random coil conformation, it will be eluted as a single sharp peak. However, under certain conditions, the native conformation and/or other intermediate conformations may also be present during the analysis. Each of these will interact differently with the stationary phase, resulting in varying retention times and multiple peaks in the chromatogram [27–33]. In some cases, irreversible conformational changes can occur by changing the temperature. Irreversible temperature-induced conformational transitions may have been responsible for the observed peak splitting of proteins under RPLC conditions [34].

Herein, short gradient runs were performed on three different column types at different temperatures. The change in the apparent gradient retention factors of antibody fragments using different stationary phases (C18 and C4, core–shell type silica based and fully porous hybrid) was investigated. The logarithm of apparent gradient retention factors $\log(k_{app})$ was plotted as a function of $1/T$. All fragments of the three different mAbs exhibited significant deviation from the conventional linear least-squared model. More surprisingly, the relationship between retention and temperature depended on the stationary phase employed. Fig 2 provides a representative example of the change in retention behavior of heavy and light chain of rituximab fragments. Experimental data shows an obvious concave curvature when $\log(k_{app})$ is plotted as a function of $1/T$, and the data can be readily fit with polynomial functions (e.g., quadratic model). The change in the retention behavior is also very similar for the heavy chain fragment on all stationary phases, whereas the light chain shows different behavior depending on the nature of the column. When using the BEH300 C4 material, the change in the retention as function of $1/T$ appears to be more linear than when using the BEH300 C18 and Aeris C18 columns. Thus, the intrinsic properties of the stationary phase (e.g., surface physicochemical properties) can play an important role at elevated temperatures. A non-linear relationship on silica-based columns is often explained by the so-called "phase transition" phenomenon [21], which is due to a conformational change in the stationary phase from a solid-like (low temperature) to a liquid-like (high temperature) state. In many cases, this transition can be diffuse and occur over a large temperature range.

A variety of phenomena may be responsible for the non-linear relationship between $\log(k)$ and $1/T$ of poly-charged analytes (mAb fragments), including: (i) possible conformational changes in the protein, (ii) changes in the dissociation rate of the functional groups with temperature and (iii) the phase transition of the stationary phase. Within the temperature range investigated (40–90 °C), the change in apparent retention factor ($\log(k_{app})$) of mAb fragments as a function of $1/T$ can be described by the quadratic models. Chromatographic optimization software commonly uses linear models for the $\log(k) - 1/T$ dependence based on two initial runs. As discussed earlier, this approach cannot be applied for the antibody fragments.

3.1.2. The effect of gradient time (gradient steepness) on the retention

In RPLC, the interaction between the stationary phase and the analyte is mediated predominantly through hydrophobic interactions between the nonpolar amino acid residues of mAbs and the immobilized n-alkyl ligands. During RPLC analysis, the gradient elution mode is preferred, wherein the solutes are eluted in order of increasing molecular hydrophobicity. Because the retention of mAbs is strongly dependent on small changes in the solvent strength, very small changes (<1%) in the organic modifier content could lead to a significant shift in the retention. Thus, isocratic conditions are impractical, and gradient elution is a requirement for the separation of real mAb samples.

In RPLC, the LSS model is the widely accepted for describing the retention of analytes as a function of the volume fraction (Φ) of the B solvent. For the gradient elution mode, the following general equation can be written:

$$\log k* = \log k_w - S\phi* \quad (2)$$

where k^* is the median value of k during gradient elution when the band has reached the column mid-point, k_w is the value of k in pure water, S is a constant for a given compound (slope of the curve) and Φ^* is the corresponding value of Φ. The dependence of k^* on the gradient time (t_g) is also typically presented, which can be described using the following equation [35,36]:

$$k* = \frac{t_g}{1.15 t_0 \Delta\phi S} \quad (3)$$

where t_0 is the column dead time. For practical reasons, modeling software such as DryLab transforms the variables of k or k^* into $\log(k)$ or $\log(k^*)$ when building a mathematical model. According to Eqs. (2) and (3), $\log(k^*)$ should exhibit a linear dependence when plotted against the logarithm of gradient time (which is related to the gradient steepness) in the case of "regular" samples.

The LSS model generally provides a good description for the retention behavior of numerous types of analytes. In some cases, deviation from a linear model can be observed. Because the conformation of proteins can vary during the elution, linear relationships cannot be used. The effect of gradient steepness (gradient time) on the retention of heavy and light chain fragments, as well as the Fab and Fc fragments, of the three mAbs was investigated. The gradient

time (steepness) was varied from 4, to 8, 12 and 16 min (at 70 and 90 °C, from 30–40% B). The retention of the fragments for all three mAbs showed very similar behavior. Fig. 3 illustrates the effect of gradient time on the retention of the heavy and light chain fragments of rituximab and the Fc and Fab fragments of bevacizumab as representative examples. In most cases, the relationship between $\log(k_{app})$ and $\log(t_g)$ can be accurately described with a linear function. Surprisingly, the retention behavior of light chains showed a slight deviation from the linear relationship. The data in the $\log(k_{app})$ versus $\log(t_g)$ plot exhibited a slight concave curvature. This behavior was most pronounced for the light chain fragments of rituximab when the temperature was set to 90 °C. Fig. 3C demonstrates the use of linear and quadratic models to fit the data. When the linear fit was employed, only two points (the two ends of the investigated gradient range, 4 min and 16 min) were considered because the modeling software only uses two experimental points when creating a linear model. For the quadratic fit, all the experimental points were taken into account. Then, retention times were modeled on the basis of two models for different gradient times (i.e., 3, 10 and 20 min). Fig. 3C demonstrates that a 1.8% difference between the predicted and observed retention times was calculated for the 3 min gradient, whereas the difference between the two models was 2.3 and 2.1% for the 10- and 20-min gradients, respectively.

In conclusion, we can confirm that the LSS model can describe the retention behavior of antibody fragments in the RP gradient elution mode within approximately 1.0–2.5% error, which is reasonable. However, when more precise prediction is required, quadratic model should be considered.

3.2. Creating a two dimensional quadratic DryLab model

The optimization software packages generally employ a linear model for the simultaneous optimization of t_g and T. The polynomial relationship of two variables can be written as:

$$y = b_0 + b_1x_1 + b_2x_2 \quad (4)$$

where y is the response (retention time or its transformation), x_1 and x_2 are the model variables, e.g., t_g and T, whereas b_0, b_1, b_2 are the model coefficients. As observed previously with antibody fragments, it is preferred to use the quadratic model to achieve maximum accuracy in the prediction of retention times. A general quadratic model for two variables can be written as:

$$y = b_0 + b_1x_1 + b_2x_2 + b_{11}x_1^2 + b_{22}x_2^2 + b_{12}x_1x_2 \quad (5)$$

The DryLab software was used for further method optimization by creating a new two dimensional mode. Retention times were transformed into retention factors, and the quadratic model was chosen for both variables (temperature and gradient time). This mode was modeled on a rectangular region in the $t_g - T$ plane determined by 3 temperature and 3 gradient times (steepness). In this case, the model requires the measurement of the effects of the variables at 3 levels. Hence, this approach is like a 3^2 factorial design, which needs 9 initial experimental runs to create a model. The gradient time was set to $tg_1 = 4$ min, $tg_2 = 8$ min and $tg_3 = 12$ min, whereas the temperature was varied from $T_1 = 70$ °C, to $T_2 = 80$ °C and $T_3 = 90$ °C. Fig. 4 shows the schematic representation of the experimental design utilized in the two-dimensional quadratic model. After performing the input experimental runs, the data (retention times, peak widths and peak tailing values) were imported into DryLab and peak tracking was performed. Subsequently, an optimization was carried out on the resolution maps, wherein the smallest resolution value (Rs) of any two critical peaks in the chromatogram was plotted as a function of two simultaneously varied experimental parameters.

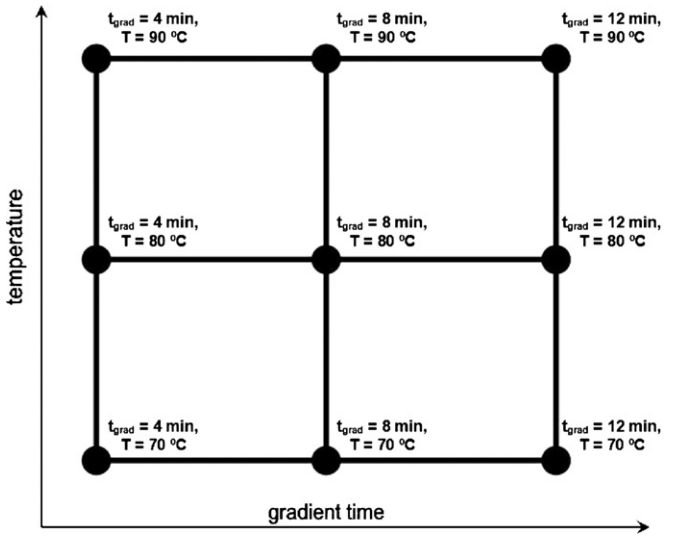

Fig. 4. Experimental design of the two-dimensional quadratic model for the optimization of mAb (IgG) fragment RPLC separation.

The accuracy of this 2 dimensional quadratic model was verified by comparing the predicted and experimentally derived chromatograms (retention times and resolution) under optimal conditions.

3.3. Accuracy of retention time and resolution predictions

3.3.1. Optimization of the separation of Fab and Fc fragments

Papain is a thiol protease that cleaves IgG antibodies at the heavy chain hinge region into three fragments: one Fc and two identical Fab fragments (Fig. 1). The separation of these domains has facilitated the investigation of the micro-heterogeneity of human monoclonal antibodies, including the confirmation of chemical and post-translational modifications, such as the N-terminal cyclization, oxidation, deamidation, and C-terminal processed lysine residues [37,38]. This study describes a fast and efficient method for the determination of variants and degradation products of a recombinant mAb (bevacizumab) from a commercial solution, using the separation power of new wide-pore core–shell type columns (Aeris Widepore of 150 mm long). The native mAb was digested with papain and the aim of the method development was to separate as many variants of the Fab and Fc fragments as possible, within the shortest achievable analysis time. Three initial gradients with different slopes were carried out at three column temperatures (as described in Section 2.3.3). Fig. 5 provides the chromatograms obtained during the 9 initial runs. Note that relatively large deviations in the peak areas (and sum of peak areas) are expected when tracking the peaks because of recovery issues with large antibody fragments at low temperatures. Moreover, the recovery of these fragments depends on their molecular weight (size). In contrast, the reproducibility of retention times, derived from consecutive runs at a constant temperature, was excellent. The result is presented in Fig. 6 as a resolution map. As shown, the 11-min gradient was found to provide the highest resolution when the column temperature was kept at 90 °C. RPLC analysis was then performed using the optimum predicted conditions, and the resulting experimental chromatograms are provided in Fig. 7, along with the predicted data.

The accuracy of the quadratic approach (using 4-, 8- and 12-min basic gradient runs with $\Delta B = 10\%$) was evaluated using the 150 mm × 2.1 mm column. The predicted and experimentally derived chromatograms (retention times and resolution) are compared in Table 1, which reveals good agreement between the

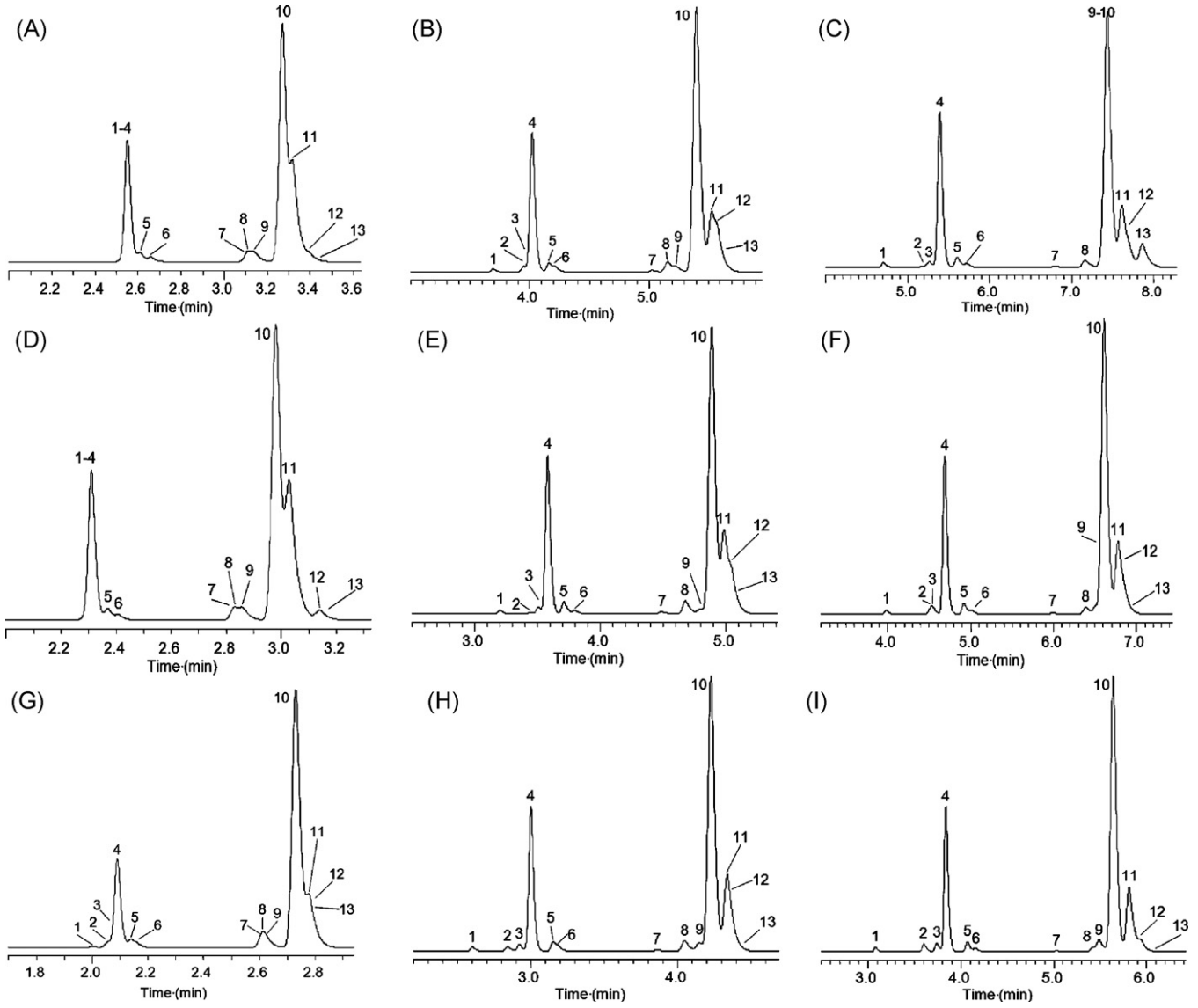

Fig. 5. Experimental chromatograms of the 9 initial runs (Bevacizumab Fc and Fab fragments). Column: Aeris WP C18 (150 mm × 2.1 mm), injected volume: 0.5 μl, detection: fluorescence (excitation at 280 nm, emission at 360 nm). Mobile phase A: 0.1% TFA in water, mobile phase B: 0.1% TFA in acetonitrile. Gradient: from 30% to 40% B, flow rate: 0.35 ml/min. Gradient time and temperature were set as 4 min, 70 °C (A), 8 min, 70 °C (B), 12 min, 70 °C (C), 4 min, 80 °C (D), 8 min, 80 °C (E), 12 min, 80 °C (F), 4 min, 90 °C (G), 8 min, 90 °C (H) and 12 min, 90 °C (I). Peaks: 1–3: pre-Fc peaks, 4: Fc, 5,6: post-Fc peaks, 7–9: pre-Fab peaks, 10: Fab, 11–13: post-Fab peaks.

Table 1
Experimental retention times and resolutions vs. predicted from the two-dimensional gradient time–temperature quadratic model of bevacizumab fragments (Fc and Fab).

Peaks	Retention time				Resolution			
	Experimental	Predicted	Difference[a]	Abs error %[b]	Experimental	Predicted	Difference[a]	Abs error %[b]
Pre-Fc 1	2.99	2.97	0.02	0.67	5.34	4.93	0.41	7.68
Pre-Fc 2	3.45	3.41	0.04	1.16	1.11	1.27	−0.16	14.41
Pre-Fc 3	3.60	3.54	0.06	1.61	0.84	0.96	−0.12	14.29
Fc	3.68	3.64	0.04	1.11	2.02	2.46	−0.44	21.78
Post-Fc 1	3.89	3.85	0.04	0.95	0.58	0.65	−0.07	12.07
Post-Fc 2	3.96	3.92	0.04	1.09	7.22	6.84	0.38	5.26
Pre-Fab 1	4.78	4.75	0.03	0.54	2.89	2.42	0.47	16.26
Pre-Fab 2	5.15	5.08	0.07	1.30	0.5	0.6	−0.10	20.00
Pre-Fab 3	5.24	5.17	0.07	1.39	0.67	0.82	−0.15	22.39
Fab	5.35	5.3	0.05	0.92	1.36	1.25	0.11	8.09
Post-Fab 1	5.49	5.45	0.04	0.75	1.01	0.57	0.44	43.56
Post-Fab 2	5.60	5.54	0.06	1.00	1.02	0.95	0.07	6.86
Post-Fab 3	5.70	5.69	0.01	0.18				
		Average		0.97		Average		16.05

[a] Difference = experimental − predicted.
[b] % error = [(experimental − predicted)/predicted] × 100.

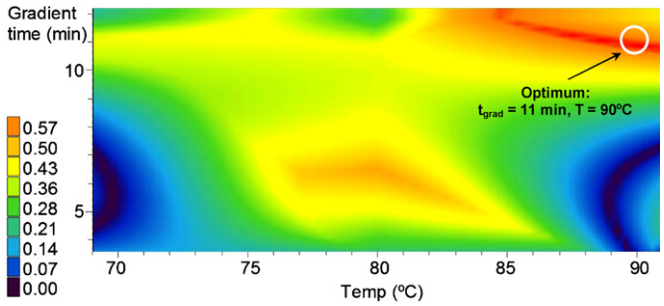

Fig. 6. Two-dimensional resolution map of the column temperature (°C) against gradient time (t_g, min) for the separation of Bevacizumab Fc and Fab fragments.

simulation and experimental results. The average relative error in the retention times was ~1.0%, which is considered an excellent prediction using such rapid gradient profiles. The mean error in the predicted resolution (*Rs*) was 16.1%. The error in the resolution values contains the retention time error as well as the uncertainty of peak width and peak symmetry prediction. Thus, this prediction is considered reliable and the suggested fast gradient runs (4, 8 and 12 min for a 150-mm long narrow bore column) can be applied in routine work, resulting in significant timesavings. In this case, the time spent for method development was approximately 8 h (3 gradient times × 3 temperatures × 3 samples). The predicted method was then experimentally verified and the final separation required only an 11-min linear gradient, whereas a separation of similar quality using conventional columns would require at least 60 min. By using the most advanced, highly efficient 150-mm long narrow bore columns, it is possible to well resolve both the Fc and the Fab variants.

3.3.2. *Optimization of the separation of light- and heavy chain fragments*

Using RPLC without enzyme digestion and under reducing conditions, the light chains (~25 kDa) can produce a single sharp peak, but the heavy chain fragments (~50 kDa) often elute as a more heterogeneous peak with slightly resolved forms. Increasing the temperature significantly improves the peak width and resolution [39]. This example illustrates the development process of a fast separation method for the resolution of light chain (LC) and heavy chain (HC) variants of a recombinant mAb (rituximab). The intact native mAb was reduced by adding DTT to the sample. Our purpose was to separate as many variants as possible with sufficient resolution. Initial gradients with different slopes were performed at three different column temperatures (as described in Section 2.3.3).

Fig. 8 provides the experimental chromatograms of the 9 basic input runs. The results are presented in the form of a resolution map in Fig. 9, which reveals that the separation performed at 81 °C using a 14-min gradient provides the highest resolution. The predicted optimum conditions were then evaluated experimentally. The results demonstrate that the predicted retention times were practically identical with those obtained experimentally, with an average error in the retention times of 0.5% (see Table 2). The resolution was also predicted with sufficient accuracy (average error of ~20%). In this manner, computer-assisted simulation can be applied with high precision for the separation of antibody fragments by using two dimensional quadratic models. Fig. 10 provides a comparison between the predicted and experimentally obtained

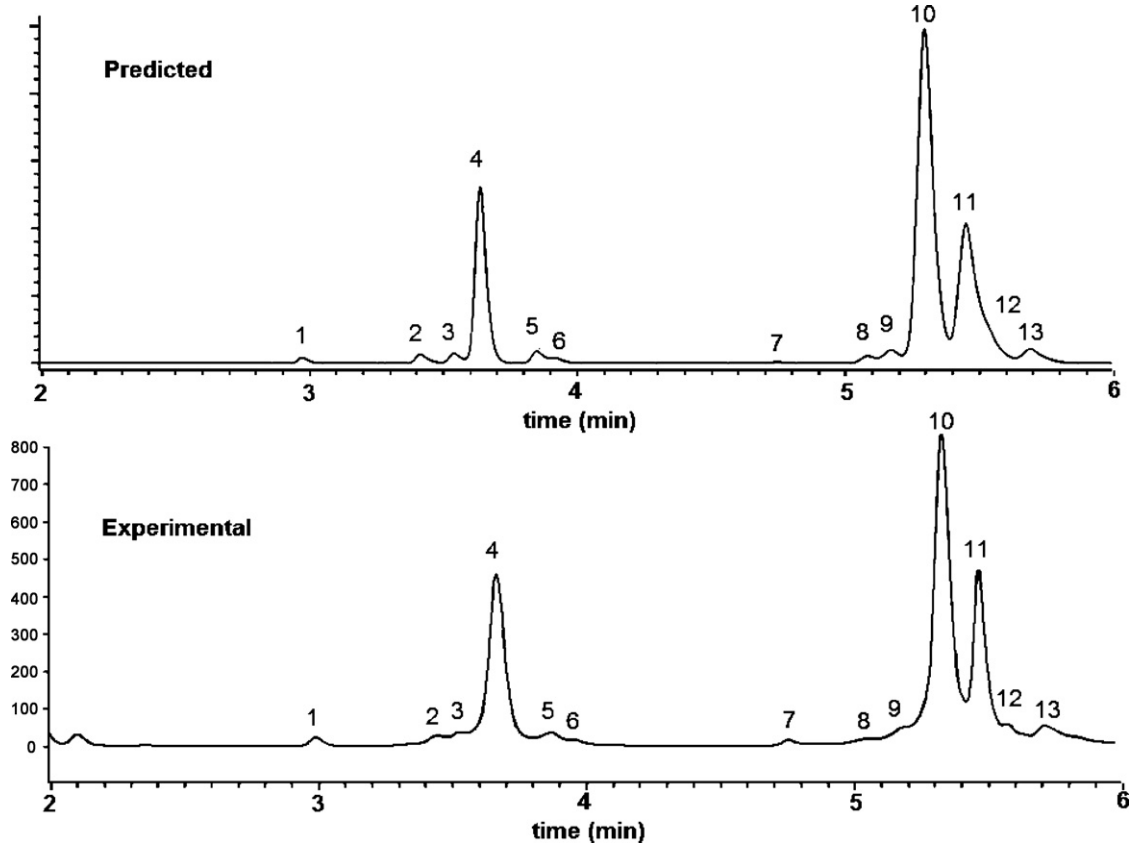

Fig. 7. Predicted and experimental chromatograms of Bevacizumab Fc and Fab fragments optimized by quadratic model. Column: Aeris WP C18 (150 mm × 2.1 mm), injected volume: 0.5 μl, detection: fluorescence (excitation at 280 nm, emission at 360 nm). Mobile phase A: 0.1% TFA in water, mobile phase B: 0.1% TFA in acetonitrile. Gradient: from 30% to 40% B, flow rate: 0.35 ml/min. Gradient time: 11 min, T = 90 °C. Peaks: 1–3: pre-Fc peaks, 4: Fc, 5,6: post-Fc peaks, 7–9: pre-Fab peaks, 10: Fab, 11–13: post-Fab peaks.

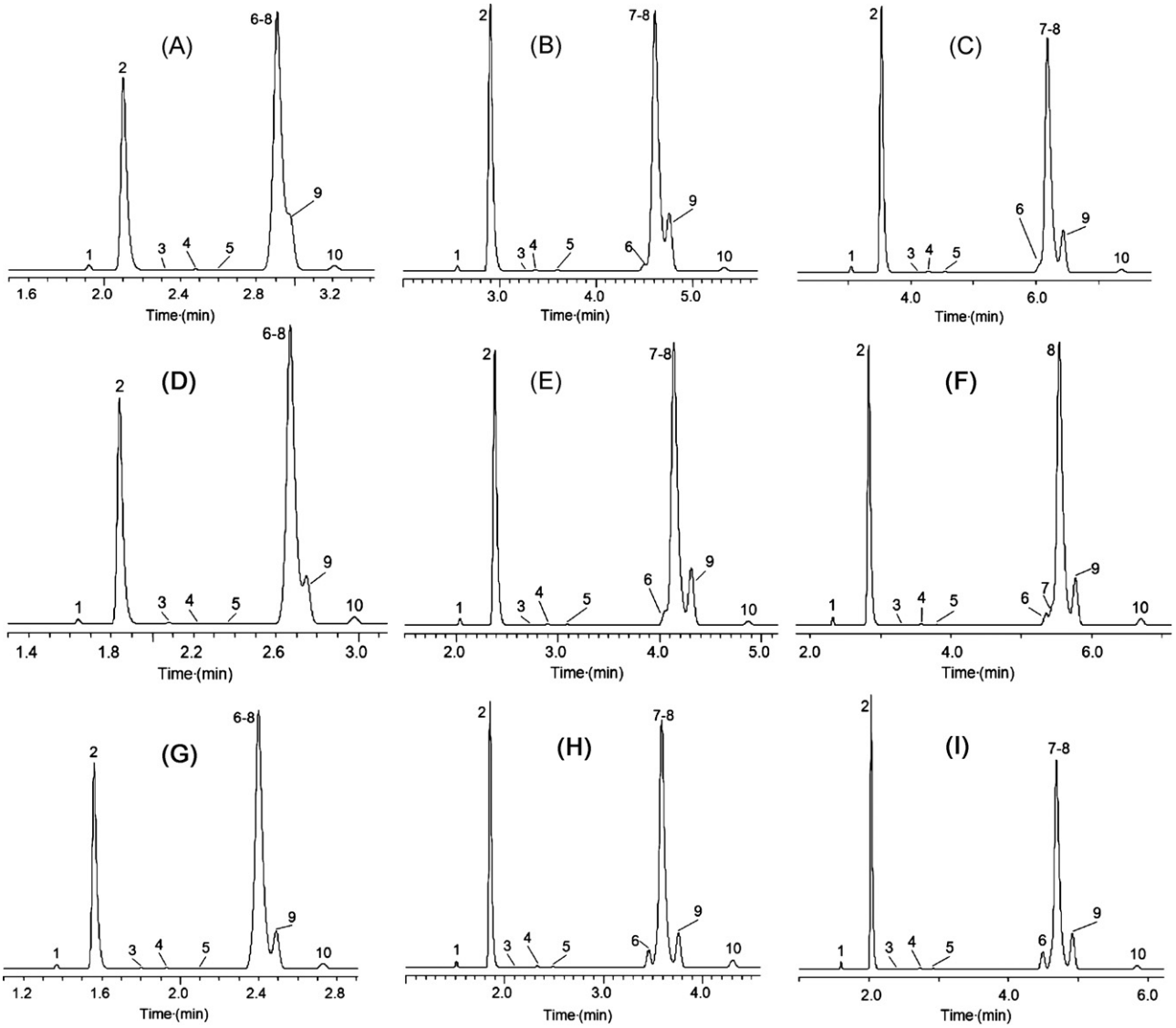

Fig. 8. Experimental chromatograms of the 9 initial runs (Rituximab LC and HC fragments). Column: Aeris WP C18 (150 mm × 2.1 mm), injected volume: 0.5 μl, detection: fluorescence (excitation at 280 nm, emission at 360 nm). Mobile phase A: 0.1% TFA in water, mobile phase B: 0.1% TFA in acetonitrile. Gradient: from 30% to 40% B, flow rate: 0.35 ml/min. Gradient time and temperature were set as 4 min, 70 °C (A), 8 min, 70 °C (B), 12 min, 70 °C (C), 4 min, 80 °C (D), 8 min, 80 °C (E), 12 min, 80 °C (F), 4 min, 90 °C (G), 8 min, 90 °C (H) and 12 min, 90 °C (I). Peaks: 1: pre-LC peak, 2: LC, 3–5: post-LC peaks, 6.7: pre-HC peaks, 8: HC, 9–10: post-HC peaks.

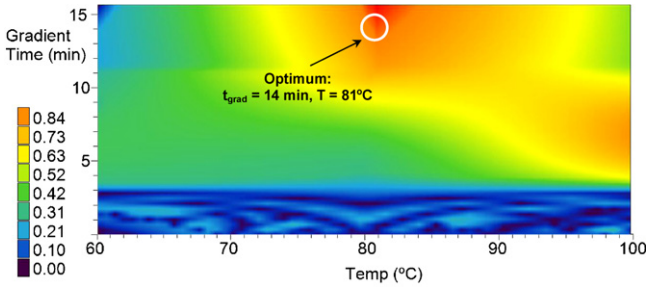

Fig. 9. Two-dimensional resolution map of the column temperature (°C) against gradient time (t_g, min) for the separation of Rituximab LC and HC fragments.

chromatograms. In this example, the method development process took was less than 6 h.

3.3.3. Comparison of quadratic and linear models

As shown in Section 3.1, the change in the retention factor (log(k)) of the antibody fragments caused by temperature ($1/T$) cannot be described accurately using linear functions, whereas the log(k_{app}) vs. gradient time log(t_g) exhibits a nearly linear correlation. Accordingly, the accuracy of the two dimensional linear and the combined linear-quadratic model were compared to that of the quadratic model. In the linear model, 4 initial runs were considered, namely: $tg_1 = 4$ min, $tg_2 = 12$ min and at $T_1 = 70$ °C, $T_2 = 90$ °C. In the combined model, 6 initial runs were considered, and the effect of gradient time was investigated at 2 levels ($tg_1 = 4$ min, $tg_2 = 12$ min), whereas the temperature was evaluated at 3 levels ($T_1 = 70$ °C, $T_2 = 80$ °C and $T_3 = 90$ °C).

By using the linear model for the example described in Section 3.3.1, the average error in the retention time prediction was 4.1%, whereas the combined model produced an average error of 1.5% (~1% error was observed with the quadratic model). For the second example (see in Section 3.3.2), the linear model produced an average error of 3.8%, whereas the combined model produced a 1.7% error for the retention time prediction (~0.5% error was observed with the quadratic model). In conclusion, the combined model can also provide acceptable accuracy (~1.5–2% error) and requires only

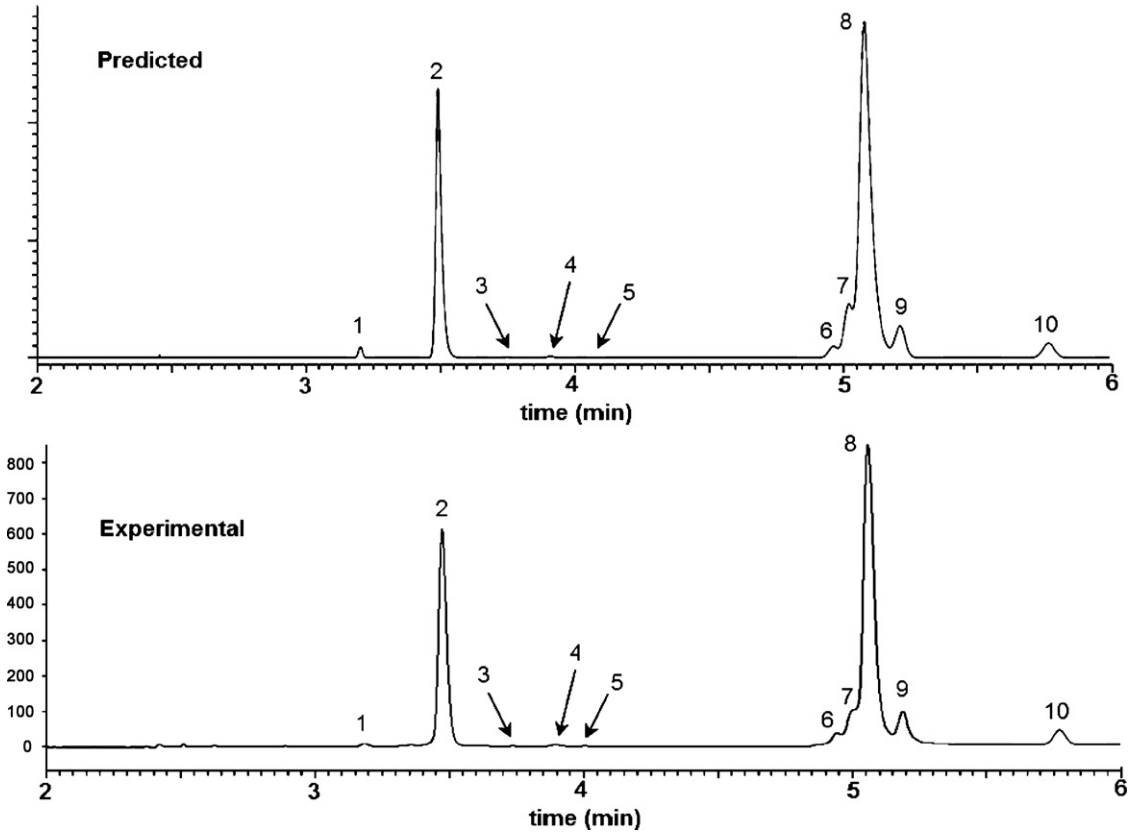

Fig. 10. Experimental and predicted chromatograms of Rituximab LC and HC fragments optimized by quadratic model. Column: Aeris WP C18 (150 mm × 2.1 mm), injected volume: 0.5 μl, detection: fluorescence (excitation at 280 nm, emission at 360 nm). Mobile phase A: 0.1% TFA in water, mobile phase B: 0.1% TFA in acetonitrile. Gradient: from 30% to 40% B, flow rate: 0.35 ml/min. Gradient time: 14 min, T = 81 °C. Peaks: 1: pre-LC peak, 2: LC, 3–5: post-LC peaks, 6.7: pre-HC peaks, 8: HC, 9–10: post-HC peaks.

Table 2
Experimental retention times and resolutions vs. predicted from the two-dimensional gradient time–temperature quadratic model of rituximab fragments (light- and heavy chain).

Peaks	Retention time				Resolution			
	Experimental	Predicted	Difference[a]	Abs error %[b]	Experimental	Predicted	Difference[a]	Abs error %[b]
Pre-LC	2.38	2.41	−0.03	1.18	6.37	8.73	−2.36	37.05
LC	2.96	2.98	−0.02	0.57	4.95	5.35	−0.40	8.08
Post-LC 1	3.49	3.5	−0.01	0.29	2.59	3.01	−0.42	16.22
Post-LC 2	3.82	3.82	0.00	0.13	1.63	2.69	−1.06	65.03
Post-LC 3	4.03	4.05	−0.02	0.45	15.21	17.04	−1.83	12.03
Pre-HC 1	5.92	5.93	−0.01	0.12	0.89	0.87	0.02	2.25
Pre-HC 2	6.06	6.04	0.01	0.25	0.75	0.87	−0.12	16.00
HC	6.15	6.14	0.01	0.18	1.79	1.41	0.38	21.23
Post-HC 1	6.41	6.43	−0.02	0.27	7.3	7.19	0.11	1.51
Post-HC 2	7.40	7.53	−0.14	1.83				
		Average		0.52		Average		19.93

[a] Difference = experimental − predicted.
[b] % error = [(experimental − predicted)/predicted] × 100.

6 initial runs. Thus, the time required for the initial runs can be shortened by a factor of 1/3 (6 runs vs. 9 runs).

4. Conclusion

The current trends in RPLC analysis of mAbs involve the use of limited fragmentation (proteolysis and reduction), which is based on the separation of the heavy and light chain variants as well as the Fab–Fc fragments. The recent advances in wide-pore columns, such as the highly efficient, fully porous sub-2 μm BEH300 or core–shell type Aeris Widepore columns, offer high resolution power for the separation of these large fragments.

Fortunately, these mAb (IgG) fragments elute in a relative narrow gradient range (e.g., 30–40% acetonitrile at elevated temperature), which means that the method optimization procedure does not require a wide range of scouting gradients (e.g., 0 to 100% B). In general, it was found that initial gradients of 30 to 40% B were appropriate for modeling the retention behavior of the fragments. In addition, it was shown previously that the use of elevated temperatures (e.g., 60–90 °C) is necessary because of recovery issues due to column adsorption of the IgG fragments. Accordingly, the effect of temperature on selectivity was investigated using a limited temperature range (e.g., 70–90 °C), eliminating the need to perform initial gradient runs at low temperatures.

In the analysis of these large analytes, deviations from the LSS and van't Hoff models appear to be critical, resulting in a decrease in the prediction accuracy. In this study, it was demonstrated that a two dimensional quadratic model and computer simulation (e.g., DryLab) can accurately predict the retention times, within an error of 1% (or lower). In addition, the optimum conditions can be determined using a very short amount of time (6–8 h).

A general 3^2 factorial design is proposed for the simultaneous optimization of gradient steepness and mobile phase temperature. The effect of these two variables should be investigated at 3 levels to construct an appropriate quadratic model. When using 150-mm long narrow bore columns, the following settings are recommended: $tg_1 = 4$ min, $tg_2 = 8$ min and $tg_3 = 12$ min (at flow rate of f = 0.35 ml/min), and the temperature should be varied from $T_1 = 70\,^{\circ}C$, to $T_2 = 80\,^{\circ}C$ and $T_3 = 90\,^{\circ}C$. The analysis of two mAb samples was used to demonstrate the reliability of this quadratic approach.

Acknowledgments

The authors wish to thank Dr Tivadar Farkas (Phenomenex Inc.) for providing the Aeris WP columns used in this study. The authors thank Róbert Berky (Budapest University of Technology and Economics, Department of Inorganic and Analytical Chemistry) for performing the DryLab calculations and providing the results.

References

[1] I. Molnár, C.s. Horváth, Separation of amino acids and peptides on non-polar stationary phases by HPLC, J. Chromatogr. 142 (1977) 623–640.
[2] I. Molnár, R.I. Boysen, V.A. Erdmann, High performance liquid chromatography of Thermus Aquaticus 50S and 30S ribosomal proteins, Chromatographia 28 (1989) 39–44.
[3] S. Fekete, J.L. Veuthey, D. Guillarme, New trends in reversed-phase liquid chromatographic separations of therapeutic peptides and proteins: theory and applications, J. Pharm. Biomed. Anal. (2012), http://dx.doi.org/10.1016/j.jpba.2012.03.024.
[4] S. Fekete, R. Berky, J. Fekete, J.L. Veuthey, D. Guillarme, Evaluation of a new wide pore core–shell material (Aeris™ WIDEPORE) and comparison with other existing stationary phases for the analysis of intact proteins, J. Chromatogr. A 1236 (2012) 177–188.
[5] S. Fekete, K. Ganzler, J. Fekete, Efficiency of the new sub-2 μm core–shell (Kinetex™) column in practice, applied for small and large molecule separation, J. Pharm. Biomed. Anal. 54 (2011) 482–490.
[6] R. Berky, S. Fekete, J. Fekete, Enhancing the quality of separation in one-dimensional peptide mapping using mathematical transformation, Chromatographia 75 (2012) 305–312.
[7] S.A. Schuster, B.M. Wagner, B.E. Boyes, J.J. Kirkland, Wider pore superficially porous particles for peptide separations by HPLC, J. Chromatogr. Sci. 48 (2010) 566–571.
[8] F. Detobel, K. Broeckhoven, J. Wellens, B. Wouters, R. Swart, M. Ursem, G. Desmet, S. Eeltink, Parameters affecting the separation of intact proteins in gradient-elution reversed-phase chromatography using poly(styrene-co-divinylbenzene) monolithic capillary columns, J. Chromatogr. A 1217 (2010) 3085–3090.
[9] S.D.R. Mould, K.R.D. Sweeney, Curr. Opin. Drug Discov. Dev. 10 (2007) 84–96.
[10] G.M. Edelman, B.A. Cunningham, W.E. Gall, P.D. Gottlieb, U. Rutishauser, M.J. Waxdal, The covalent structure of an entire gamma G immunoglobulin molecule, J. Immunol. 173 (2004) 5335–5342.
[11] N. Lundell, T. Schreitmuller, Sample preparation for peptide mapping—a pharmaceutical quality-control perspective, Anal. Biochem. 266 (1999) 31–47.
[12] K.R. Williams, K.L. Stone, Identifying sites of posttranslational modifications in proteins via HPLC peptide mapping, Methods Mol. Biol. 40 (1995) 157–175.
[13] S. Fekete, J. Fekete, I. Molnár, K. Ganzler, Rapid high performance liquid chromatography method development with high prediction accuracy, using 5 cm long narrow bore columns packed with sub-2 μm particles and design space computer modelling, J. Chromatogr. A 1216 (2009) 7816–7823.
[14] R.M. Krisko, K. McLaughlin, M.J. Koenigbauer, C.E. Lunte, Application of a column selection system and DryLab software for high-performance liquid chromatography method development, J. Chromatogr. A 1122 (2006) 186–193.
[15] J.A. Lewis, L.R. Snyder, J.W. Dolan, Initial experiments in high-performance liquid chromatographic method development II. Recommended approach and conditions for isocratic separation, J. Chromatogr. A 721 (1996) 15–29.
[16] J.W. Dolan, L.R. Snyder, N.M. Djordjevic, D.W. Hill, D.L. Saunders, L. Van Heukelem, T.J. Waeghe, Simultaneous variation of temperature and gradient steepness for reversed-phase high-performance liquid chromatography method development: I. Application to 14 different samples using computer simulation, J. Chromatogr. A 803 (1998) 1–31.
[17] L.R. Snyder, J.J. Kirkland, J.L. Glajch, Practical HPLC Method Development, second ed., John Wiley & Sons Inc., 1997.
[18] J.C. Berridge, Techniques for the Automated Optimization of HPLC Separations, John Wiley & Sons, New York, 1986.
[19] S. Fekete, S. Rudaz, J.L. Veuthey, D. Guillarme, Impact of mobile phase temperature on recovery and stability of monoclonal antibodies using recent reversed-phase stationary phases, J. Sep. Sci., http://dx.doi.org/10.1002/jssc.201200297, in press.
[20] D. Guillarme, D.T.T. Nguyen, S. Rudaz, J.L. Veuthey, Method transfer for fast liquid chromatography in pharmaceutical analysis: application to short columns packed with small particle. Part II: gradient experiments, Eur. J. Pharm. Biopharm. 68 (2008) 430–440.
[21] S. Heinisch, J.-L. Rocca, Sense and non-sense of high-temperature liquid chromatography, J. Chromatogr. A 1216 (2009) 642–658.
[22] W.R. Melander, J. Stoveken, C.s. Horváth, Mobile phase effects in reversed-phase chromatography: II. Acidic amine phosphate buffers as eluents, J. Chromatogr. 185 (1979) 111–127.
[23] C.B. Castells, C. Rafols, M. Roses, E. Bosch, Effect of temperature on the chromatographic retention of ionizable compounds: I. Methanol–water mobile phases, J. Chromatogr. A 1042 (2004) 23–35.
[24] Y. Chen, C.T. Mant, R.S. Hodges, Temperature selectivity effects in reversed-phase liquid chromatography due to conformation differences between helical and non-helical peptides, J. Chromatogr. A 1010 (2003) 45–61.
[25] C.T. Mant, Y. Chen, R.S. Hodges, Temperature profiling of polypeptides in reversed-phase liquid chromatography: I. Monitoring of dimerization and unfolding of amphipathic α-helical peptides, J. Chromatogr. A 1009 (2003) 29–43.
[26] C.T. Mant, B. Tripet, R.S. Hodges, Temperature profiling of polypeptides in reversed-phase liquid chromatography: II. Monitoring of folding and stability of two-stranded α-helical coiled-coils, J. Chromatogr. A 1009 (2003) 45–59.
[27] S.A. Cohen, K. Benedek, Y. Tapuhi, J.C. Ford, B.L. Karger, Conformational effects in the reversed phase liquid chromatography of ribonuclease A, Anal. Biochem. 144 (1985) 275–284.
[28] X.M. Lu, K. Benedek, B.L. Karger, Conformational effects in the high-performance liquid chromatography of proteins. Further studies of the reversed-phase chromatographic behavior of ribonuclease A, J. Chromatogr. 359 (1986) 19–29.
[29] P. Oroszlan, S. Wicar, G. Teshima, S.-L. Wu, W.S. Hancock, B.L. Karger, Conformational effects in the reversed-phase chromatographic behavior of recombinant human growth hormone (rhGH) and N-methionine recombinant human growth hormone (Met-hGH), Anal. Chem. 64 (1992) 1623–1631.
[30] A.W. Purcell, M.I. Aguilar, M.T.W. Hearn, Probing the conformational states of proteins with reversed phase high performance liquid chromatography, Anal. Chem. 71 (1999) 2440–2451.
[31] S.U. Sane, S.M. Cramer, T.M. Przybycien, Protein structure perturbations on chromatographic surfaces, J. Chromatogr. A 849 (1999) 149–159.
[32] S. Wicar, M.G. Mulkerrin, G. Bathory, L.H. Khundkar, B.L. Karger, Conformational changes in the reversed phase liquid chromatography of recombinant human growth hormone as a function of organic solvent: the molten globule state, Anal. Chem. 66 (1994) 3908–3915.
[33] K. Sawicka, T. Sahota, M.J. Taylor, S. Tanna, Development of a reversed-phase high-performance liquid chromatography method for the analysis of components from a closed-loop insulin delivery system, J. Chromatogr. A 1132 (2006) 117–123.
[34] A.W. Purcell, M.I. Aguilar, M.T.W. Hearn, Conformational effects in reversed-phase high-performance liquid chromatography of polypeptides I. Resolution of insulin variants, J. Chromatogr. A 711 (1995) 61–70.
[35] J.W. Dolan, L.R. Snyder, Developing a gradient elution method for reversed-phase HPLC, LC–GC 5 (1988) 970–978.
[36] L.R. Snyder, Gradient elution, in: C. Horvath (Ed.), HPLC: Advances and Perspectives, vol. 1, Academic Press, New York, 1980, pp. 208–316.
[37] B. Yan, J. Valliere-Douglass, L. Brady, S. Steen, M. Han, D. Pace, S. Elliott, Z. Yates, A. Balland, W. Wang, D. Pettit, Analysis of post-translational modifications in recombinant monoclonal antibody IgG1 by reversed-phase liquid chromatography/mass spectrometry, J. Chromatogr. A 1164 (2007) 153–161.
[38] G. Kleemann, J. Beierle, A. Nichols, T. Dillon, G. Pipes, P. Bondarenko, Characterization of IgG1 immunoglobulins and peptide-Fc fusion proteins by limited proteolysis in conjunction with LC–MS, Anal. Chem. 80 (2008) 2001–2009.
[39] Q. Zhao, T.A. Stadheim, L. Chen, M.W. Washabaugh, Molecular and functional characterization of monoclonal antibodies, in: Z. An (Ed.), Therapeutic Monoclonal Antibodies, John Wiley & Sons, Inc., Hoboken, NJ, 2009, pp. 525–540.